AD-A156 851 ALTERNATIVE COORDINATE SYSTEMS FOR HIGH LATITUDE IONOSPHERIC PLASMA STUDI..(U) MISSION RESEARCH CORP SANTA BARBARA CA D J MALOOF ET AL. 15 MAR 83 MRC-R-816 1/1

UNCLASSIFIED DNA-TR-84-56 DNA001-82-C-0089 F/G 20/14 NL

END
DATE
FILMED
9 85

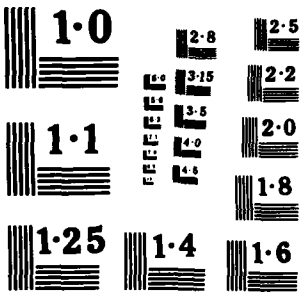
1·0
2·8
2·5
3·15
2·2
3·5
2·0
1·1
1·8
1·25
1·4
1·6

AD-A156 851

(2)

DNA-TR-84-56

ALTERNATIVE COORDINATE SYSTEMS FOR HIGH LATITUDE IONOSPHERIC PLASMA STUDIES

D.J. Maloof
W.W. White
Mission Research Corp
P.O. Drawer 719
Santa Barbara, CA 93102-0719

15 March 1983

Technical Report

CONTRACT No. DNA 001-82-C-0089

APPROVED FOR PUBLIC RELEASE;
DISTRIBUTION UNLIMITED.

THIS WORK WAS SPONSORED BY THE DEFENSE NUCLEAR AGENCY
UNDER RDT&E RMSS CODE B322083466 S99QMXBC00083 H2590D.

Prepared for
Director
DEFENSE NUCLEAR AGENCY
Washington, DC 20305-1000

DTIC
ELECTE
JUL 23 1985
S D
B

DTIC FILE COPY

85 5 03 063

Destroy this report when it is no longer needed. Do not return to sender.

PLEASE NOTIFY THE DEFENSE NUCLEAR AGENCY, ATTN: STTI, WASHINGTON, DC 20305-1000, IF YOUR ADDRESS IS INCORRECT, IF YOU WISH IT DELETED FROM THE DISTRIBUTION LIST, OR IF THE ADDRESSEE IS NO LONGER EMPLOYED BY YOUR ORGANIZATION.

UNCLASSIFIED

SECURITY CLASSIFICATION OF THIS PAGE (When Data Entered)

REPORT DOCUMENTATION PAGE		READ INSTRUCTIONS BEFORE COMPLETING FORM
1. REPORT NUMBER DNA-TR-84-56	2. GOVT ACCESSION NO. AD-A156 851	3. RECIPIENT'S CATALOG NUMBER
4. TITLE (and Subtitle) ALTERNATIVE COORDINATE SYSTEMS FOR HIGH LATITUDE IONOSPHERIC PLASMA STUDIES		5. TYPE OF REPORT & PERIOD COVERED Technical Report May 82 - Mar 83
		6. PERFORMING ORG. REPORT NUMBER MRC-R-816
7. AUTHOR(s) D. J. Maloof W. W. White		8. CONTRACT OR GRANT NUMBER(s) DNA 001-82-C-0089
9. PERFORMING ORGANIZATION NAME AND ADDRESS Mission Research Corporation P. O. Drawer 719 Santa Barbara, CA 93102-0719		10. PROGRAM ELEMENT, PROJECT, TASK AREA & WORK UNIT NUMBERS Task S99QMXBC-00083
11. CONTROLLING OFFICE NAME AND ADDRESS Director Defense Nuclear Agency Washington, DC 20305		12. REPORT DATE 15 March 1983
		13. NUMBER OF PAGES 62
14. MONITORING AGENCY NAME & ADDRESS(if different from Controlling Office)		15. SECURITY CLASS (of this report) UNCLASSIFIED
		15a. DECLASSIFICATION/DOWNGRADING SCHEDULE N/A since UNCLASSIFIED

16. DISTRIBUTION STATEMENT (of this Report)

Approved for public release; distribution unlimited.

17. DISTRIBUTION STATEMENT (of the abstract entered in Block 20, if different from Report)

18. SUPPLEMENTARY NOTES

This work was sponsored by the Defense Nuclear Agency under RDT&E RMSS Code B322083466 S99QMXBC00083 H2590D.

19. KEY WORDS (Continue on reverse side if necessary and identify by block number)

High Latitude Ionosphere
Polar Ionosphere
Magnetosphere
Nuclear Phenomenology
High Altitude Nuclear Explosions

20. ABSTRACT (Continue on reverse side if necessary and identify by block number)

Detailed numerical calculations which attempt to model the electromagnetic coupling between the polar ionosphere and the solar wind driven magnetospheric current systems must be formulated with a recognition of the wide range of physical scale sizes which must be accommodated within the constraint of finite computer resources. This is especially true of a numerical calculation which attempts to include the effects of high altitude nuclear explosion generated disturbances in the polar ionosphere.

DD FORM 1 JAN 73 1473 EDITION OF 1 NOV 65 IS OBSOLETE

UNCLASSIFIED

SECURITY CLASSIFICATION OF THIS PAGE (When Data Entered)

20. ABSTRACT (Continued)

For this problem it is necessary to resolve simultaneously both "small" scale features (~ 100 km or less in extent) in the ionosphere and "large" scale features of the magnetosphere (features with dimensions greater than the radius of the earth). If standard coordinate systems are used, a computational grid which spans the magnetosphere will contain an unacceptably large number of cells. This report describes a unique coordinate system, the "zeta coordinate system", which was developed to circumvent this problem. The zeta coordinate system has the property of being approximately aligned with a dipole magnetic field in the near-earth zone, but it transitions smoothly to approach a cylindrical coordinate system far from the earth. This coordinate system is specified by simple analytic expressions.

Accession For
NTIS GRA&I ☑
DTIC TAB ☐
Unannounced ☐
Justification
By
Distribution/
Availability Codes
Dist | Avail and/or Special
A-1

SUMMARY

The problem of formulating an orthogonal, analytic (i.e., non-numerical) coordinate system for use in a simulation of the coupled ionosphere/magnetosphere/solar wind system which has been perturbed by a high altitude nuclear explosion at high magnetic latitude has been investigated. Experience with existing MHD codes, which simulate the behavior of mid-latitude ionospheric plasmas, indicates that a very useful coordinate system to use in such studies is one which is aligned with the geomagnetic field. Unfortunately, the presence of magnetospheric field-aligned current systems precludes the possibility of constructing an analogous orthogonal magnetic-field-aligned coordinate system suitable for the high latitude problem. It is possible, however, to characterize an interesting class of possible orthogonal coordinate functions which generalize the formal structure of the dipole-field-aligned coordinate system in a mathematically simple way. One member of this class - referred to above as the "zeta-coordinate system" - has been studied in considerable detail. This coordinate system is dipolar in character at small distances from the origin but becomes cylindrical at larger distances. It can, therefore, be used to generate computational meshes which appear to be better tailored to the requirements of the high latitude problem than those which can be generated using standard coordinate systems. The zeta-coordinate system is double-valued. The nature of this double-valuedness can be specified quite precisely, however, and does not seem to offer an impediment to the use of this coordinate system in practical applications.

TABLE OF CONTENTS

Section		Page
	SUMMARY	1
	LIST OF ILLUSTRATIONS	3
1	INTRODUCTION	5
2	SOME PRELIMINARY CONCEPTS	13
3	A CLASS OF POSSIBLE COORDINATE FUNCTIONS	17
4	A SPECIAL COORDINATE SYSTEM	31
	REFERENCES	43
	APPENDIX	45

LIST OF ILLUSTRATIONS

Figure		Page
1	A schematic view of the earth's magnetosphere.	7
2	ζ_1 and ζ_2 contours for $k^{1/3} = 6\ R_e$.	36
3	An illustration of the use of two azimuthal axes in generating a mesh based upon the ζ-coordinate system.	39
3a	The portion of the mesh of Figure 2 which lies within the circle of radius $k^{1/3}$.	39
3b	The portion of the mesh of Figure 2 which lies outside the circle of radius $k^{1/3}$.	39
3c	An example of how Figures 3a and 3b might be rejoined to generate a complete mesh.	40
A-1	Horner's Method applied to the polynomial $\tilde{P}(R)$.	51
A-2	Horner's Method applied to the polynomial $\tilde{\tilde{P}}(R)$.	52

SECTION 1
INTRODUCTION

For the past several years, the Defense Nuclear Agency (DNA) has been pursuing a research program to develop a comprehensive understanding of the phenomenology of high altitude nuclear explosions. The motivation for this effort has been a recognition, spawned in the early 1960s by high altitude nuclear tests (over the mid-Pacific near Johnston Island)[1], that nuclear explosions at ionospheric altitudes could produce widespread and long lasting detrimental effects upon radio communication links, radars, and optical or IR sensors. In addition, such explosions can disrupt the operation of electrical equipment through the phenomenon of electromagnetic pulse (EMP). In the 1970s, the primary emphasis of DNA's research was directed toward effects at low and mid latitudes (low latitudes because all of the high altitude nuclear tests were conducted at magnetic L-shells of about two or less, mid latitudes because of the location of CONUS). The scope of current research efforts includes examinations of existing data from atmospheric nuclear tests, theoretical efforts to develop new understandings which go beyond available data, and non-nuclear experiments.

As the overall picture of high altitude nuclear phenomenology has become more complete, the DNA community has shifted from simply trying to sort out gross effects to developing a refined picture of high altitude nuclear explosions and the manner in which they interact with their surrounding environment. With this evolution in thinking has come a recognition that the high altitude environment at high magnetic latitudes (the auroral oval and polar cap regions) is, in a number of respects, quite different from that at mid and low latitudes.

PREVIOUS PAGE IS BLANK

From the nuclear weapons effects point of view, the uniqueness of the high latitude ambient environment stems from the departure, at polar latitudes, of the earth's magnetic field from a dipolar geometry. (Refer to Figure 1.) The key issues are the physical processes which are linked to the highly distorted geomagnetic field. At low and mid magnetic latitudes (L-shells of ~12 or less), the field lines are closed and fairly closely approximate dipole field lines. These field lines lie within the plasmapause and are shielded by the magnetosphere from direct exposure to the solar wind. In contrast, magnetic field lines originating in the polar regions (high L-shells) extend out into (and perhaps through) the magnetosphere where they are exposed to the influences of the solar wind. At high latitudes, energy delivered to the magnetosphere by the solar wind can be transferred to the polar ionosphere by electrical currents which descend along polar magnetic field lines from the magnetosheath. These are the Birkeland currents.[2] Studies[3] by specialists in the theory of current driven plasma instabilities suggest that these currents, which are unique to high latitude field lines, may drive plasma instabilities which lead to ionospheric structure at scale sizes which can affect radio and radar transmissions over a broad frequency spectrum. This ionospheric plasma structure may bear similarity to field-aligned structure which develops in plasmas produced by high altitude nuclear explosions.

In recognition of the significance of such naturally occurring effects, and in view of the direct connection of such effects to the high altitude nuclear phenomenology problem, DNA has undertaken a research program to acquire in-situ data at polar latitudes. The program has included the WIDEBAND Satellite Program[4] and, more recently, the HILAT Satellite Program.[5] Each of these programs involved/involves active ionospheric probes from polar orbiting spacecraft. DNA has also pursued theoretical efforts to understand the basic phenomenology leading to disturbances in the ambient ionospheric environment and to understand the connections of the physics of that phenomenology to the nuclear effects

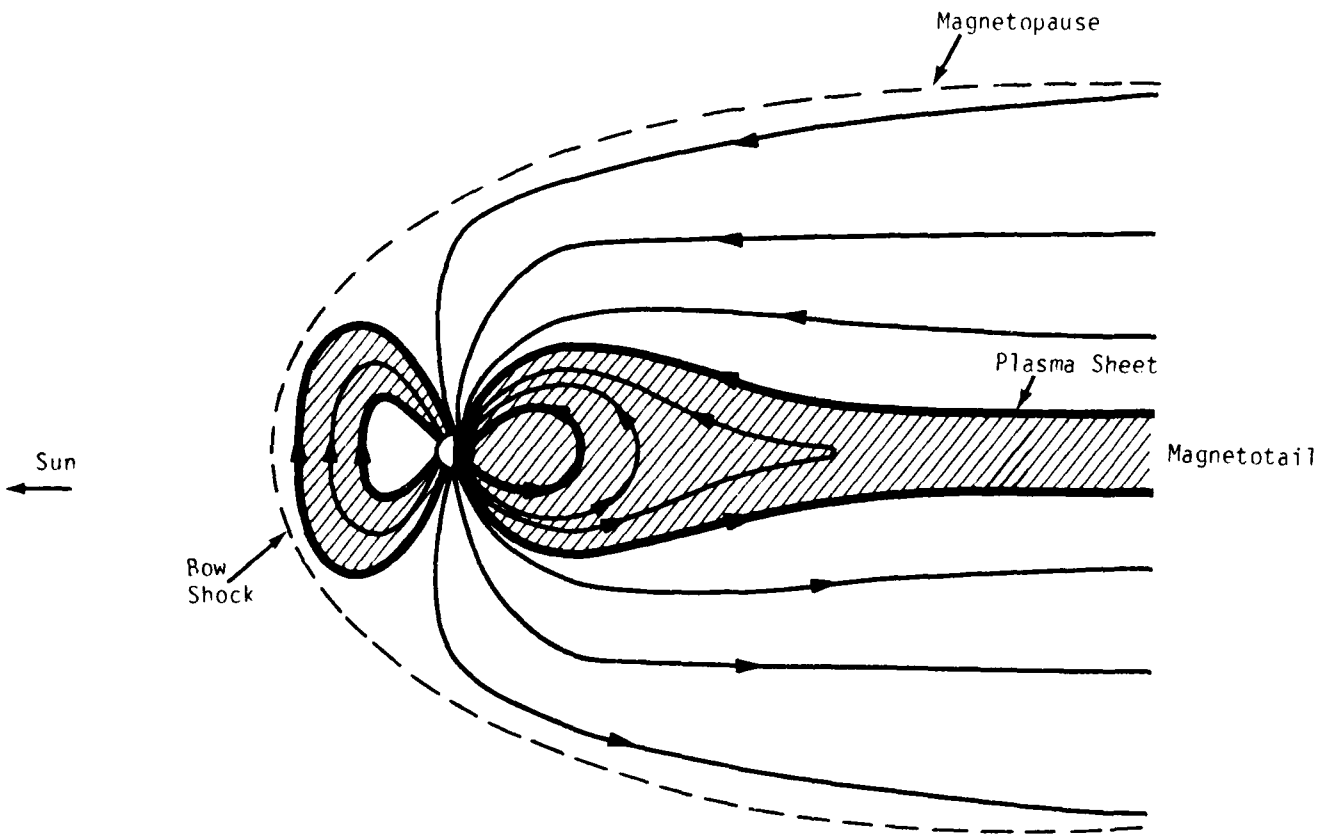

Figure 1. A schematic view of the earth's magnetosphere.

problem. Data from the WIDEBAND satellite and the associated theoretical interpretations of that data have had a direct influence on the current state of understanding of propagation effects resulting from structured plasma environments.[6] A similar wealth of information from the HILAT satellite is anticipated.

There are other reasons to be interested in high latitude phenomenology. Note that the solar wind energy flux incident on the magnetosphere is equivalent to ~10 KT/hour to ~10 MT/hour, depending on the state of magnetic activity. Under naturally occurring conditions, only a small fraction of this energy flux is directly coupled into the magnetosphere system. However, it has been suggested that a high altitude nuclear explosion at polar latitudes could possibly alter the ambient magnetospheric current patterns in such a way as to deliver over a broad area of the polar ionosphere an energy input equivalent to perhaps megatons per hour of additional nuclear explosions.[7] The sources of this energy would be twofold: i) energy stored in the current systems within the magnetosphere, and ii) energy delivered to the magnetosphere by the solar wind and directly transmitted to the polar ionosphere. The proposed initiator of this process and conduit for the energy flux is the nuclear plume, a magnetic-field-aligned column of high density plasma created by a high altitude nuclear explosion, which may reach several tens of thousands of kilometers from the polar ionosphere up into the magnetospheric currents.

At present, this concept has not been explored by theoretical or experimental means. The equations which are thought to describe the coupled ionosphere/magnetosphere/solar wind system under ambient conditions are complex, and the magnetic field geometry in which these equations need to be solved is formidable. In addition, the extra complications introduced by a high altitude nuclear explosion render the nuclear effects problem quite difficult.

A first step in attacking this problem is to develop a suitable framework in which to perform calculations. Due to the complexity of the problem, it is assumed that the theoretical approach will involve numerical calculations. This report describes a specialized, three dimensional, orthogonal coordinate system which has been developed for the purpose of numerically modeling the earth's magnetosphere and the interaction of high altitude nuclear explosions with magnetospheric currents. Because the magnetosphere spans an incredible volume by terrestrial standards, and because numerical simulations of it must treat, with some sensible degree of spatial resolution, features with a wide range of characteristic scale sizes, the well known coordinate systems (Cartesian, cylindrical, and spherical) are easily shown to present formidable problems. If one wants to resolve simultaneously "fine scale" features near the earth (e.g., Birkeland currents and associated ionospheric processes), some measure of detail in the bow shock and magnetopause regions (e.g., coupling mechanisms by which solar wind energy is transferred to the magnetospheric current systems), and very large gradient length features associated with the tail region (which stretches many tens of earth radii in the antisunward direction), then a coordinate system/computational grid combination with enough flexibility to distribute grid points or cells in an appropriate fashion with economy of computer resources is required.

When one sets out to design a computational grid within which to model the magnetosphere, one rapidly finds that direct application of the well known coordinate systems leads to an enormous number of grid cells which far exceeds the high speed memory capacity of any present-day computer. Furthermore, none of these coordinate systems naturally matches all of the boundary surfaces or important features of the magnetosphere. For example, the spherical coordinate system is ideal for modeling the ionosphere and features near the earth (provided one makes it a geocentric coordinate system), but far from the earth, spherical coordinate surfaces don't match the shape of the outer portions of the magnetosphere or con-

without loss of generality. This is the required conclusion. To establish the second part of Theorem 2, suppose $R_1''=0$ so that $R_1 = r+a_1$, modulo an irrelevant multiplicative constant. The analysis above remains valid up to and including Equation (3-16), but now it is possible that k_3 does not vanish. Assume this happens. Then none of the k_i's can vanish. Using Equations (3-9) and (3-10) one obtains

$$\frac{R_2'}{R_2} = k_1 \left(\frac{r + a_1}{r^2}\right) \tag{3-27a}$$

and

$$\frac{R_3'}{R_3} = k_2 \left(\frac{r + a_1}{r^2}\right) . \tag{3-27b}$$

Inserting these expressions into Equation (3-12) results in

$$k_1 k_2 \left(\frac{r + a_1}{r}\right)^2 = k_3 \tag{3-28}$$

Since this true for all r, a_1 must vanish. To determine Φ_2 and Φ_3, use Equation (3-13):

$$\frac{\Phi_3'}{\Phi_3} = - k_4 \frac{\Phi_2}{\Phi_2'} \tag{3-29}$$

or

$$\Phi_3 = e^{-k_4 \int d\phi \frac{\Phi_2}{\Phi_2'}} . \tag{3-30}$$

Note that Equation (3-13) is the only constraint upon the functions Φ_i so that Φ_2 is arbitrary here. Without loss of generality, then, one may redefine $\Phi_2 \to \Phi_2^{k_1}$. This leads to

$$\frac{R_2'}{R_2} = \frac{k_1 R_1}{r^2 R_1'} \tag{3-21}$$

or

$$R_2 = e^{k_1 \int \frac{R_1 \, dr}{r^2 R_1'}} \tag{3-22}$$

up to an irrelevant multiplicative constant. Also

$$\frac{\Theta_2'}{\Theta_2} = k_1 \cot \theta \tag{3-23}$$

or

$$\Theta_2 = \sin^{k_1}\theta \ . \tag{3-24}$$

By Equation (3-11), R_3 and Θ_3 are both constant. To determine Φ_2 and Φ_3 consider Equation (3-13b). One of Φ_2' and Φ_3' must vanish. If Φ_3' vanishes then the ζ's no longer define a three dimensional coordinate system, so that, in fact Φ_2' must vanish. Thus, Φ_2 must be constant, leaving Φ_3 arbitrary. To summarize, it has been shown that

$$\zeta_2 = \left[e^{\int \frac{R_1 \, dr}{r^2 R_1'}} \sin \theta\right]^{k_1} \tag{3-25a}$$

$$\zeta_3 = \Phi_3(\phi) \tag{3-25b}$$

up to irrelevant constants. Again arguments given in Section 2 imply that ζ_2 and ζ_3 may be defined by

$$\zeta_2 = e^{\int \frac{R_1 \, dr}{r^2 R_1'}} \sin \theta \tag{3-26a}$$

and

$$\zeta_3 = \phi \tag{3-26b}$$

The requirement $R_1'' \neq 0$ may now be used to show that $k_3 = 0$. From (3-9b) and (3-10b)

$$\frac{R_2'}{R_2}\frac{R_3'}{R_3} = k_1 k_2 \left(\frac{R_1}{r^2 R_1'}\right)^2 . \tag{3-17}$$

Substituting into (3-12b), there results

$$\frac{k_1 k_2}{r^2}\left(\frac{R_1}{R_1'}\right)^2 = k_3 \tag{3-18}$$

or

$$\sqrt{k_1 k_2}\, R_1 = \sqrt{k_3}\, r R_1' . \tag{3-19}$$

Differentiating both sides and using (3-16), this becomes

$$\sqrt{k_3}\, R_1' = \sqrt{k_3}\, R_1' + \sqrt{k_3}\, r R_1'' \tag{3-20}$$

which implies $k_3 = 0$ since $R_1'' \neq 0$. Of course, (3-16) now also implies that k_3, k_4 and $k_1 k_2$ all vanish. From (3-9), (3-10), and (3-11) k_1 and k_2 cannot both vanish, however, for then $\{R_i', \Theta_i', \Phi_i'\}$ would vanish for one of $i = 2$ or 3. This would mean that ζ_i = constant for $i = 2$ or 3, and $\{\zeta_i\}$ would no longer define a three dimensional coordinate system. Thus, there are two alternatives.

Either $k_2 = k_3 = k_4 = 0$ with $k_1 \neq 0$ or $k_1 = k_3 = k_4 = 0$ with $k_2 \neq 0$. The symmetry of form present in Equations (3-9) and (3-10) implies that the coordinate systems determined by each of these alternatives are the same - one may consider only the first alternative without loss of generality. From Equation (3-9) then

and

$$\frac{r^2 R_2' R_3'}{R_2 R_3} + \frac{\Theta_2' \Theta_3'}{\Theta_2 \Theta_3} + \frac{1}{\sin^2\theta} \frac{\Phi_2' \Phi_3'}{\Phi_2 \Phi_3} = 0 \ . \tag{3-11}$$

Equation (3-11) in turn implies

$$r^2 \frac{R_2' R_3'}{R_2 R_3} = - \left[\frac{\Theta_2' \Theta_3'}{\Theta_2 \Theta_3} + \frac{1}{\sin^2\theta} \frac{\Phi_2' \Phi_3'}{\Phi_2 \Phi_3}\right] \tag{3-12a}$$

$$= k_3 \ . \tag{3-12b}$$

The right hand side of Equation (3-12) may also be separated

$$\sin^2\theta \left(\frac{\Theta_2' \Theta_3'}{\Theta_2 \Theta_3} + k_3\right) = - \frac{\Phi_2' \Phi_3'}{\Phi_2 \Phi_3} \tag{3-13a}$$

$$= k_4 \ . \tag{3-13b}$$

All the k_i above are at this stage arbitrary constants. The proof is completed by showing that some of these constants must vanish and by using this information to delimit the form of the various derivatives occurring above. Multiplying (3-9) by (3-10) one obtains

$$\frac{\Theta_2' \Theta_3'}{\Theta_2 \Theta_3} = k_1 k_2 \cot^2\theta \ . \tag{3-14}$$

Substituting this expression into (3-13a) results in

$$\sin^2\theta \left[k_1 k_2 \cot^2\theta + k_3\right] = k_4 \ . \tag{3-15}$$

The validity of Equation (3-15) for arbitrary θ implies the following important relationship among the separation constants

$$k_3 = k_4 = k_1 k_2 \ . \tag{3-16}$$

Also

$$\nabla\zeta_1 \cdot \nabla\zeta_3 = R_1' R_3' \cos\theta\, \Theta_3\, \Phi_3 - \frac{1}{r^2} R_1 R_3 \sin\theta\, \Theta_3'\, \Phi_3 \tag{3-7}$$

$$= 0 ,$$

and

$$\nabla\zeta_2 \cdot \nabla\zeta_3 = R_2' R_3' \Theta_2 \Theta_3 \Phi_2 \Phi_3 + \frac{1}{r^2} R_2 R_3 \Theta_2' \Theta_3' \Phi_2 \Phi_3 \tag{3-8}$$

$$+ \frac{1}{r^2 \sin^2\theta} R_2 R_3 \Theta_2 \Theta_3 \Phi_2' \Phi_3'$$

$$= 0 .$$

Dividing both sides of (3-6) by $\{\frac{R_1 R_2}{r^2} \cos\theta\, \Theta_2\, \Phi_2\}$ and noting that if a function of r alone is equal to a function of θ alone for all r and θ, then these two functions must both be equal to a constant, one obtains

$$\frac{r^2 R_1' R_2'}{R_1 R_2} = \tan\theta \frac{\Theta_2'}{\Theta_2} \tag{3-9a}$$

$$= k_1 . \tag{3-9b}$$

Similarly, (3-7) and (3-8) imply respectively

$$\frac{r^2 R_1' R_3'}{R_1 R_3} = \tan\theta \frac{\Theta_3'}{\Theta_3} \tag{3-10a}$$

$$= k_2 \tag{3-10b}$$

if $R_1'' \neq 0$. (Here the primes imply differentiation.) If $R_1'' = 0$, then the following set of coordinate functions is the only additional possibility:

$$\zeta_1 = r \cos \theta \ , \tag{3-4a}$$

$$\zeta_2 = r \sin \theta \ \Phi_2(\phi) \ , \tag{3-4b}$$

and

$$\zeta_3 = r \sin \theta \ e^{-\int \frac{\Phi_2 d\phi}{\Phi_2'}} \ .$$

Here $\Phi_2(\phi)$ is an arbitrary function such that $\Phi_2' \neq 0$.

Proof: The proof is accomplished by using the orthogonality requirement to develop a system of simultaneous partial differential equations for the R_i, Θ_i and Φ_i. These equations may then be solved in terms of a set of separation constants k_j to obtain the required result. Proceeding then, the orthogonality requirement

$$\nabla\zeta_i \cdot \nabla\zeta_j = 0 \ , \qquad i \neq j \ , \tag{3-5}$$

implies

$$\begin{aligned} \nabla\zeta_1 \cdot \nabla\zeta_2 &= R_1' R_2' \cos \theta \ \Theta_2 \ \Phi_2 \\ &\quad - \frac{1}{r^2} R_1 R_2 \sin \theta \ \Theta_2' \ \Phi_2 \qquad (3\text{-}6) \\ &= 0 \ . \end{aligned}$$

SECTION 3
A CLASS OF POSSIBLE COORDINATE FUNCTIONS

In this section, two results will be presented regarding the possibility of formally generalizing the mathematical structure of the dipole-field-aligned coordinate system described in Section 2. Many possible generalizations might be explored. However, for the sake of analytic tractability, attention here will be restricted to coordinate functions of the form

$$\zeta = R(r)\ \Theta(\theta)\ \Phi(\phi) \tag{3-1}$$

where r, θ, ϕ are the usual spherical coordinates. Coordinate functions of this form will be referred to as "separable coordinate functions." We present two important theorems.

Theorem 2

The most general set of "separable coordinate functions," including the coordinate function

$$\zeta_1 = R_1(r) \cos \theta \tag{3-2}$$

and satisfying the requirements of orthogonality, is given by

$$\zeta_1 = R_1(r) \cos \theta\ , \tag{3-3a}$$

$$\zeta_2 = e^{\int \frac{R_1 dr}{r^2 R_1'}} \sin \theta\ , \tag{3-3b}$$

and

$$\zeta_3 = \phi \tag{3-3c}$$

Thus, a magnetic field $\vec{B}$, obeying the usual Maxwell equations, cannot possess a pseudo-potential unless $\vec{B} \cdot \vec{J}_{total}$ vanishes, where $\vec{J}_{total}$ is the total current associated with $\vec{B}$. Therefore, the field-aligned currents in the magnetosphere prohibit the existence of a field-aligned coordinate system.

Even though the presence of field aligned currents forbids the existence of an orthogonal coordinate system aligned with the magnetospheric $\vec{B}$ field, it may be still possible to design a coordinate system which is more faithful to the particulars of the earth-solar wind geometry than one of the standard coordinate systems. Such a coordinate system might, for example possess a dipolar or spherical character near the surface of the earth but transition to a more cylindrical behavior at large distances from the earth in order to conform to the elongated configuration of the magnetosphere (c.f. Figure 1). The remainder of this report is dedicated to an exploration of this idea.

coordinate system defined by Equations (2-4) permits a ready decomposition of the plasma motion into components which are either parallel or transverse to this magnetic field. Experience has shown that such a decomposition is crucial in simulating the detailed aspects of plasma behavior relevant to high altitude nuclear phenomenology while meeting the constraints of available computer resources.

Given this experience, it seems appropriate to begin attacking the problem with which this report is concerned by asking whether or not it is possible to construct an orthogonal coordinate system aligned with the non-dipolar, solar-wind-distorted magnetic field of the earth's magnetosphere (c.f. Figure 1). Interestingly enough, it can be demonstrated that the presence of field-aligned currents within the magnetosphere rigorously precludes the possibility of such a construction. The validity of this statement is directly implied by the following necessary condition for the vector field $\vec{F}(\vec{r})$ to possess a pseudo-potential.[9]

Theorem 1

If the vector field $\vec{F}(\vec{r})$ has a pseudo-potential $\Psi(\vec{r})$, then $\vec{F} \cdot \nabla x \vec{F}$ must vanish.

Proof: $\vec{F} \cdot \nabla x \vec{F}$

$$= \mu(\vec{r})\ \nabla\Psi \cdot \nabla x\, \mu(\vec{r}) \nabla\Psi \qquad (2\text{-}6)$$

$$= \mu(\vec{r})\ \nabla\Psi \cdot [\nabla\mu(\vec{r})\ x\ \nabla\Psi + \mu(\vec{r})\ \nabla x \nabla\Psi] \qquad (2\text{-}7)$$

$$= 0$$

for some i. If Equation (2-3) holds, $\mu(\vec{r})$ is said to be an integrating factor and ζ_i a pseudo-potential for the field $\vec{F}$.

An interesting example of these ideas, important for MHD simulations of mid-latitude ionospheric plasmas, is the geomagnetic-dipole-field-aligned coordinate system. This coordinate system is defined by the coordinate functions* α, β, γ:

$$\cos \alpha = \left(\frac{R_e}{R}\right)^2 \cos \theta \ , \tag{2-4a}$$

$$\sin \beta = \left(\frac{R_e}{R}\right)^{1/2} \sin \theta \ , \tag{2-4b}$$

and

$$\gamma = \phi \ . \tag{2-4c}$$

Here, R_e is the radius of the earth and (R, θ, ϕ) are geocentric spherical coordinates with the colatitude θ being measured from the geomagnetic pole. α, β, and γ satisfy the orthogonality conditions (2-2). In addition, it may be easily verified that the gradient of α is proportional to the geomagnetic dipole field, $\vec{B}_{dipole}$, given by

$$\vec{B}_{dipole} = -.31 \left(\frac{R_e}{R}\right)^3 \left[2 \cos \theta \, \hat{r} + \sin \theta \, \hat{\theta}\right] \ \text{(gauss)} \tag{2-5}$$

where $\hat{r}$ and $\hat{\theta}$ are radial and colatitudinal unit vectors. For an ionospheric plasma moving in the dipole magnetic field of the earth, the

---

* Notice that the sets of coordinate functions $\{\xi_i\}$ and $\{f_i(\xi_i)\}$ (no sum on i) describe equivalent coordinate systems since the gradient of ξ_i and that of $f_i(\xi_i)$ are parallel. This freedom of definition has been used in Equations (2.4) to define coordinate functions α, β, γ which are measured in radians.

SECTION 2
SOME PRELIMINARY CONCEPTS

As a prelude to a detailed discussion of the problem with which this report is concerned, it may be useful to review a few basic definitions regarding the concept of a coordinate system. Following Reference 9, a coordinate system is a threefold family of surfaces with defining equations

$$\zeta_i(\vec{r}) = (\text{constant})_i \ , \qquad 1 \leq i \leq 3 \ , \tag{2-1}$$

which may be inverted to yield $\vec{r}$ as a function of the ζ_i's. The ζ_i's are referred to as coordinate functions and the intersection of two of the surfaces defined in (2-1) is called a coordinate line. The coordinate system defined by $\{\zeta_i\}$ $(\equiv \{\zeta_1, \zeta_2, \zeta_3\})$ is said to be orthogonal if

$$\nabla\zeta_i \cdot \nabla\zeta_j = 0 \ , \qquad i \neq j \ . \tag{2-2}$$

In practice, the property of orthogonality is an important simplifying feature of a coordinate system. For this reason, as stated in the introduction, only orthogonal coordinate systems will be considered in this report. One last concept which should be mentioned at this point is that of a field-aligned coordinate system. A coordinate system $\{\zeta_i\}$ is said to be aligned with a vector field $\vec{F}(\vec{r})$ if $\nabla\zeta_i$ is parallel to $\vec{F}$ for some i. This means that there must exist a scalar function $\mu(\vec{r})$ such that

$$\mu(\vec{r})\ \nabla\zeta_i = \vec{F}(\vec{r}) \tag{2-3}$$

Given that the unusual geometry of the magnetosphere is a cause for difficulty, one might be tempted by the idea of a magnetic-field-aligned coordinate system. This approach will be explained later in this report. The idea is quite attractive, but as will be shown, the differential geometry of such an idea is incompatible with the physics of the magnetosphere.

The coordinate system developed in this report, the "zeta coordinate system", has been designed to have desirable geometric properties in the near-earth region (i.e., it can match selected features in and above the ionosphere) and to transition gracefully to a coordinate system which allows for simple exterior boundary surfaces. The coordinate surfaces of this system can be made to conform closely to dipolar surfaces near the earth (so they look like a field-aligned system there). These coordinates retain enough flexibility to permit the user to orient the dipole axis arbitrarily relative to the earth-sun axis. Far from the earth, the coordinate system approaches a cylindrical system with the axis along the earth-sun direction. The zeta coordinate system is orthogonal.

The following sections of this report explain the theoretical basis for this coordinate system. In Section 2, a brief review of some basic mathematical concepts relevant to the study of coordinate systems is presented. In Section 3, an attempt is made to generalize the mathematical form of the dipole-field-aligned coordinate system[8] which has been used previously for modeling low and mid latitude nuclear effects. This results in a simple characterization of an interesting class of possible coordinate functions. Next, in Section 4, one member of this class, the zeta coordinate system, is examined. This system is well suited to performing simulations of magnetospheric physics. Finally, the results are summarized in Section 5.

farther in the antisunward direction than in the sunward direction without any problem. However, near the earth the coordinate surfaces do not match the geometry of the ionosphere. In order to resolve details in the ionosphere, the cylindrical cells must be relatively small (~50 km on a side, for example). Direct extension of the resulting cylindrical coordinate surfaces to magnetospheric distances leads to a large number of computational cells which are much smaller than is appropriate. This means that one must resort to numerical "fixes" to try to make the simulation physically sensible in an important portion of the problem (the ionosphere), subject to the constraint of a limited computer memory (i.e., a limited number of grid cells).

A third candidate is Cartesian coordinates. The situation is similar to that of cylindrical coordinates. Far from the earth, the boundary conditions are easily implemented, but near the earth, coordinate surfaces do not match the natural geometry of the problem. Closely spaced coordinate surfaces near the earth translate into excessive numbers of unnecessarily small grid cells well out into the magnetosphere.

It is worth noting that so far only orthogonal coordinate systems have been considered. This has been deliberate. In order to insure that the differential or integral equations that are to be solved to simulate the magnetosphere remain tractable, we have chosen to require orthogonality of any candidate coordinate system. Experience has shown that the effort required to implement on a computer complex equations in a nonorthogonal coordinate system can become unreasonably large. In addition, we impose the requirement that the candidate coordinate system be analytically generated. This requirement allows one to perform a fair amount of exploration of the physics equations before going to the computer.

form to the streamlines of the solar wind. If one wants the bounding surfaces of the computational space to be simple coordinate surfaces (spherical in this case), then a grid which extends well out into the magnetotail (say 40 earth radii) will also extend well out (40 earth radii to be exact) in the sunward direction. Unfortunately, that means slightly less than half of the entire grid volume will lie sunward of the bow shock in the zone of unperturbed solar wind. For many problems, this situation represents a tremendous waste of computer resources (storage and central processor time). This problem can be overcome by programming the computer to chop out or ignore grid cells in uninteresting regions, but only at the expense of computer code simplicity.

Also note that if one wants spatial resolution of 2 earth radii, for example, at a distance of 20 earth radii, the angular separation of radial grid lines needs to be 0.1 radians. Therefore, in a simple-minded application of spherical geometry, these radial lines define cells in the ionosphere which have dimensions on the order of 650 km -- far too large to be useful. Conversely, choosing the cell dimensions and radial coordinate surface spacing according to ionospheric criteria leads to numerous cells at large distances from the earth which are inappropriately small.

These considerations lead to the conclusion that spherical coordinates are not particularly well suited to the magnetospheric problem. Numerical calculations in a spherical coordinate system would require substantial effort just to define an acceptable computational grid.

It is appropriate to next investigate cylindrical coordinates. Assume the cylindircal axis lies along the earth-sun line. (The reader may wish to convince himself that other orientations are of limited utility, at best.) Then boundary conditions far from the earth (outside the magnetosphere) are simple to implement, and the grid can be extended much

$$\Phi_3 = e^{-k_4 \int d\phi \frac{\Phi_2}{k_1 \Phi_2'}} \tag{3-31a}$$

$$= e^{-k_2 \int d\phi \frac{\Phi_2}{\Phi_2'}} . \tag{3-31b}$$

Summarizing, the following expression for the ζ_i are implied by the equations above:

$$\zeta_1 = r \cos \theta , \tag{3-32a}$$

$$\zeta_2 = (r \sin \theta \, \Phi_2)^{k_1} , \tag{3-32b}$$

and

$$\zeta_3 = (r \sin \theta \, e^{-\int d\phi \frac{\Phi_2}{\Phi_2'}})^{k_2} , \tag{3-32c}$$

which is equivalent to the desired result.

Theorem 3

The only set of coordinate functions $\{\zeta_i\}$ satisfying orthogonality and separability and such that

$$\zeta_1 = R_1(r) \sin \theta \cos \phi \tag{3-33}$$

is the set of cartesian coordinate functions.

Proof: The orthogonality and separability requirements may be used as in Theorem 2 to develop a system of simultaneous partial differential equations. These equations are then solved in terms of a set of separation

constants to show that one of the coordinate functions must have the form $R(r) \cos \theta$ so that Theorem 3 follows as a corollary of Theorem 2. To proceed with the proof, note that the orthogonality criteria are

$$\begin{aligned} \nabla\zeta_1 \cdot \nabla\zeta_2 &= R_1' R_2' \sin\theta\, \Theta_2 \cos\phi\, \Phi_2 \\ &+ \frac{1}{r^2} R1\, R2 \cos\theta\, \Theta_2' \cos\phi\, \Phi_2 \\ &- \frac{1}{r^2 \sin^2\theta} R_1 R_2 \sin\theta\, \Theta_2 \sin\phi\, \Phi_2' \\ &= 0 , \end{aligned} \tag{3-34}$$

$$\begin{aligned} \nabla\zeta_1 \cdot \nabla\zeta_3 &= R_1' R_3' \sin\theta\, \Theta_3 \cos\phi\, \Phi_3 \\ &+ \frac{1}{r^2} R_1 R_3 \cos\theta\, \Theta_3' \cos\phi\, \Phi_3 \\ &- \frac{1}{r^2 \sin^2\theta} R_1 R_3 \sin\theta\, \Theta_3 \sin\phi\, \Phi_3' \\ &= 0 , \end{aligned} \tag{3-35}$$

and

$$\begin{aligned} \nabla\zeta_2 \cdot \nabla\zeta_3 &= R_2' R_3' \Theta_2 \Theta_3 \Phi_2 \Phi_3 \\ &+ \frac{1}{r^2} R_2 R_3 \Theta_2' \Theta_3' \Phi_2 \Phi_3 \\ &+ \frac{1}{r^2 \sin^2\theta} R_2 R_3 \Theta_2 \Theta_3 \Phi_2' \Phi_3' \\ &= 0 . \end{aligned} \tag{3-36}$$

From (3-34) and (3-35)

$$\frac{r^2 R_1' R_i'}{R_1 R_i} + \frac{\Theta_i'}{\Theta_i} \cot \theta - \frac{1}{\sin^2 \theta} \frac{\Phi_i'}{\Phi_i} \tan \phi = 0 \tag{3-37}$$

for $i = 2, 3$. This implies

$$\frac{r^2 R_1' R_i'}{R_1 R_i} = k_i \tag{3-38}$$

and

$$\frac{\Theta_i'}{\Theta_i} \cot \theta - \frac{\tan \phi}{\sin^2 \theta} \frac{\Phi_i'}{\Phi_i} = - k_i \ . \tag{3-39}$$

Equation (3-39) may be separated to produce

$$[\frac{\Theta_i'}{\Theta_i} \cos \theta + k_i \sin \theta] \sin \theta = k_{2+i} \tag{3-40}$$

and

$$\frac{\Phi_i'}{\Phi_i} \tan \phi = + k_{2+i} \ . \tag{3-41}$$

Turning to Equation (3-36) one finds

$$\frac{r^2 R_2' R_3'}{R_2 R_3} + \frac{\Theta_2' \Theta_3'}{\Theta_2 \Theta_3} + \frac{\Phi_2' \Phi_3'}{\sin^2\theta \ \Phi_2 \Phi_3} = 0 \ . \tag{3-42}$$

This implies

$$\frac{r^2 R_2' R_3'}{R_2 R_3} = k_6 \tag{3-43}$$

and

$$\frac{\Theta_2' \Theta_3'}{\Theta_2 \Theta_3} + \frac{\Phi_2' \Phi_3'}{\sin^2\theta \, \Phi_2 \Phi_3} = - k_6 \, . \tag{3-44}$$

The last equation may be further separated to produce

$$\left(\frac{\Theta_2' \Theta_3'}{\Theta_2 \Theta_3} + k_6\right) \sin^2\theta = - k_7 \tag{3-45}$$

and

$$\frac{\Phi_2' \Phi_3'}{\Phi_2 \Phi_3} = + k_7 \, . \tag{3-46}$$

The above equations can now be solved for the various k_j and the required result obtained. First, note that Equation (3-41) implies

$$\frac{\Phi_2' \Phi_3'}{\Phi_2 \Phi_3} \tan^2\phi = k_5 k_4 \tag{3-47}$$

With the help of Equation (3-46) this becomes

$$k_7 \tan^2\phi = k_5 k_4 \tag{3-48}$$

which implies

$$k_7 = 0$$

and (3-49)

$$k_5 k_4 = 0 \, .$$

Thus, by Equation 3-46, one of $\frac{\Phi_2'}{\Phi_2}$, $\frac{\Phi_3'}{\Phi_3}$ must vanish. Suppose $\frac{\Phi_2'}{\Phi_2} = 0$. Then, by Equations (3-39) and (3-38)

$$\frac{\Theta_2'}{\Theta_2} = - k_2 \tan \theta \tag{3-50}$$

and

$$\frac{R_2'}{R_2} = \frac{k_2 R_1}{r^2 R_1'} \quad . \tag{3-51}$$

Clearly, k_2 cannot vanish if $\{\zeta_i\}$ is to define a three dimensional coordinate system. The above equations imply

$$\zeta_2 = \left[e^{\int \frac{dr\, R_1}{r^2 R_1'}} \cos \theta\right]^{k_2} \tag{3-52}$$

or equivalently

$$\zeta_2 = e^{\int dr \frac{R_1}{r^2 R_1'}} \cos \theta \ . \tag{3-53}$$

Given the non-trivial ϕ dependence hypothesized of ζ_1, Theorem 2 forces

$$\zeta_1 = r \sin \theta \cos \phi \ , \tag{3-54a}$$

$$\zeta_2 = r \cos \theta \ , \tag{3-54b}$$

and

$$\zeta_3 = r \sin \theta \sin \phi \ . \tag{3-54c}$$

A similar result follows if one takes $\frac{\Phi_3'}{\Phi_3} = 0$. This is the desired conclusion.

Theorems 2 and 3 rather severely limit the extent to which it is possible to generalize the dipolar field aligned coordinate system in the manner described in Section 2, using separable orthogonal coordinates. To see this, note that such a generalization must involve one coordinate function $\zeta_1(\vec{r})$, say, which satisfies

$$\zeta_1(\vec{r}) \to V_{dipole} = \frac{\vec{p} \cdot \vec{r}}{r^3} \quad \text{for values of } r \sim R_{earth} \tag{3-55}$$

Here, $\vec{p}$ is the moment vector associated with the dipole field to which the coordinate system involving ζ_1 is aligned in the near earth region. Now

$$\vec{p} \cdot \vec{r} = p_1 r \sin\theta \cos\phi + p_2 r \sin\theta \sin\phi + p_3 r \cos\theta \tag{3-56}$$

In order for the coordinate function ζ_1 to be separable, $\vec{p}_i = p_i \hat{e}_i$ for some particular i. If i = 1 or 2, then Theorem 3 implies that ζ_1 must be part of a cartesian system and so cannot become dipolar for any value of r. If i = 3, then Theorem 2 completely fixes the set of coordinate functions to which ζ_1 belongs once the radial dependence of ζ_1 is specified.

In what follows, the coordinate system resulting from the choice of ζ_1 given by

$$\zeta_1 = (r - kr^{-n}) \cos\theta \tag{3-57}$$

for arbitrary non-zero constants k and n will be investigated with particular emphasis upon the case n = 2. For large r and positive n, ζ_1 approaches the Cartesian coordinate z. For small r and n = 2, ζ_1 approaches the dipole coordinate cos α. Note that the spherical surface

of radius $k^{\frac{1}{n+1}}$, centered at the origin is a surface of constant ζ_1. Thus, the orthogonal coordinate system including $\zeta_1(\vec{r})$ also possesses the qualitative features of a spherical coordinate system for a certain range of $\vec{r}$.

SECTION 4
A SPECIAL COORDINATE SYSTEM

The complete specification of the set of orthogonal coordinate functions to which ζ_1 (Equation 3-57) belongs can be accomplished by using Theorem 2. To do this, the following indefinite integral must be evaluated.

$$\int dr \left[\frac{(r-kr^{-n})}{r^2\ (1+nkr^{-n-1})}\right] \tag{4-1a}$$

$$= \int dr\left[-\frac{1}{nr} + \left(\frac{n+1}{n}\right)\frac{r^n}{r^{n+1} + kn}\right] \tag{4-1b}$$

$$= \ln\left[(r^n + kn/r)^{1/n}\right] + \text{irrelevant constant} \ . \tag{4-1c}$$

Inserting this expression into Equations (3-3) above, the following coordinate functions are obtained:

$$\zeta_1 = (r - kr^{-n})\cos\theta \ , \tag{4-2a}$$

$$\zeta_2 = (r^n + nkr^{-1})^{1/n}\sin\theta \ , \tag{4-2b}$$

and

$$\zeta_3 = \phi$$

Specializing to the case n=2, Equations (4-2) become

$$\zeta_1 = (r - k/r^2) \cos \theta \ , \tag{4-3a}$$

$$\zeta_2 = \sqrt{(r^2 + 2k/r)} \sin \theta \ , \tag{4-3b}$$

and

$$\zeta_3 = \varsigma \ . \tag{4-3c}$$

As a check, the orthogonality condition

$$\nabla\zeta_i \cdot \nabla\zeta_j = 0 \ , \quad i \neq j \ , \tag{4-4}$$

may be explicitly verified by computing the gradients of the ζ_i above:

$$\nabla\zeta_1 = (1 + \frac{2k}{r^3}) \cos \theta \ \hat{r} - (1 - k/r^3) \sin \theta \ \hat{\theta} \ , \tag{4-5a}$$

$$\nabla\zeta_2 = \frac{(r - k/r^2)}{\sqrt{r^2 + 2k/r}} \sin \theta \ \hat{r} + \frac{1}{r} \ \sqrt{(r^2 + 2k/r)} \cos \theta \ \hat{\theta} \ , \tag{4-5b}$$

and

$$\nabla\zeta_3 = \frac{1}{r \sin \theta} \ \hat{\phi} \ . \tag{4-5c}$$

While the orthogonality of the coordinate system defined by $\{\zeta_i\}$ is guaranteed by Theorem 2, the question of <u>invertibility</u> of this coordinate system, i.e., of whether or not the specification of $(\zeta_1, \zeta_2, \zeta_3)$ uniquely determines (r, θ, ϕ), has yet to be addressed. In order to treat this question, it is useful to consider two separate cases: $\zeta_1 = 0$ and $\zeta_1 \neq 0$.

$\underline{\zeta_1=0}$

In this case, by Equations 4-3, there are two alternatives. Either:

$$r = k^{1/3} , \tag{4-6a}$$

$$\theta = \sin^{-1} \left(\frac{\zeta_2}{\sqrt{3}\ k^{1/3}}\right) , \tag{4-6b}$$

and

$$\phi = \zeta_3 \tag{4-6c}$$

or

$$\theta = \pm \pi/2 , \tag{4-7a}$$

$$r^3 - \zeta_2^2 r + 2k = 0 , \tag{4-7b}$$

and

$$\phi = \zeta_3 . \tag{4-7c}$$

The "or" here is of course an inclusive "or", and the sign of θ is the same as the sign of ζ_2. The branch of this alternative which obtains for a given triple $(0,\zeta_2,\zeta_3)$ (and, hence, the answer to the question of invertibility) is determined by the magnitude of ζ_2. If $|\zeta_2| > \sqrt{3}\ k^{1/3}$, then Equation (4-6b) has no real solution so that Equations (4-7) must be used. The radial variable r is then determined by the positive roots of Equation (4-7b). As discussed in the Appendix, these roots are two in number. One is always less than $k^{1/3}$ and the other is always greater than the $k^{1/3}$. They are given explicitly by[10]

$$r_1 = \frac{2}{\sqrt{3}} |\zeta_2| \cos A \tag{4-8a}$$

and

$$r_2 = \frac{2}{\sqrt{3}} |\zeta_2| \cos(A + \frac{4\pi}{3}) \tag{4-8b}$$

with

$$A = \frac{1}{3} \cos^{-1}\left[\frac{-3\sqrt{3}\ k}{\zeta_2^3}\right] . \tag{4-8c}$$

Thus, the ζ coordinate system is not strictly invertible for $\zeta_1=0$, and $|\zeta_2| > \sqrt{3}\ k^{1/3}$. On the other hand, if $|\zeta_2| < \sqrt{3}\ k^{1/3}$, then Equation (4-7b) has no real roots (c.f. Equation 4-8c), so the use of Equations (4-6) is necessitated. These equations yield unique values of (r, θ, ϕ), thus insuring invertibility for $\zeta_1=0$ and $|\zeta_2| < \sqrt{3}\ k^{1/3}$. Finally, if $|\zeta_2| = \sqrt{3}\ k^{1/3}$, then Equations (4-6) and Equations (4-7) give the same unique result, namely $r = k^{1/3}$, $\theta = \pm \pi/2$.

$\underline{\zeta_1 \neq 0}$

In analyzing this case, it is useful to begin by isolating the theta dependance in Equations (4-2a) and (4-2b):

$$\frac{\zeta_1}{r - k/r^2} = \cos\ \theta , \tag{4-9a}$$

$$\frac{\zeta_2}{\sqrt{r^2 + 2k/r}} = \sin\ \theta , \tag{4-9b}$$

Squaring both sides of each equation and adding the results, there follows

$$\frac{\zeta_1^2\ r^4}{(r^3 - k)^2} + \frac{\zeta_2^2\ r}{r^3 + 2k} = 1 . \tag{4-10}$$

This expression can be simplified by multiplying both sides by $(r^3-k)^2\ (r^3+2k)$, expanding the various products which arise, and collecting powers of r. Equation (4-10) then becomes

$$P(r) \equiv r^9 - (\zeta_1^2+\zeta_2^2)r^7 - 2k(\zeta_1^2-\zeta_2^2)r^4 - 3k^2r^3 - k^2\zeta_2^2 r + 2k^3$$

$$= 0 \ . \qquad (4\text{-}11)$$

Equation (4-11) implictly determines r for given ζ_1 and ζ_2 in terms of the (positive) roots of a ninth order polynominal P(r). Unfortunately, the complexity of Equation (4-11) appears to render dubious the prospect of obtaining explicit analytic expressions for these roots as was done above for the case $\zeta_1=0$. It is possible, however, to determine rigorously the number of positive roots of P(r) and to obtain upper and lower bounds upon each of these roots without benefit of such explicit knowledge. This is done in detail in the Appendix, using certain theorems from the theory of equations. Therein, it is shown that P(r) has precisely two positive roots for $\zeta_1 \neq 0$. One of these lies in the interval $(0, k^{1/3})$ and the other in the interval $(k^{1/3}, k^{1/3} + \sqrt{M})$ where

$$M \equiv \max\left[(\zeta_1^2+\zeta_2^2),\ 2(\zeta_1^2-\zeta_2^2),\ 3k^{2/3}\right] \qquad (4\text{-}12)$$

Thus the ζ-coordinate system is double valued for non-vanishing values of ζ_1, just as it is for $\zeta_1=0$, $\zeta_2>\sqrt{3}\ k^{1/3}$.

Even though the ζ-coordinate system is not strictly invertible, as shown above, the lack of invertibility is of a sufficiently innocuous form that this coordinate system may still be used in practical application. It is simply necessary to specify a parameter which distinguishes between the inside and outside of the sphere of radius $k^{1/3}$, in addition to the triple $(\zeta_1, \zeta_2, \zeta_3)$. Then the polynomial P(r) can be numerically solved for a <u>unique</u> value of r, either lying in the interval $(0, k^{1/3})$ or in the interval $(k^{1/3}, k^{1/3} + \sqrt{M})$. A mesh which has been generated using this technique is shown in Figure 2. The value of $k^{1/3}$ which has

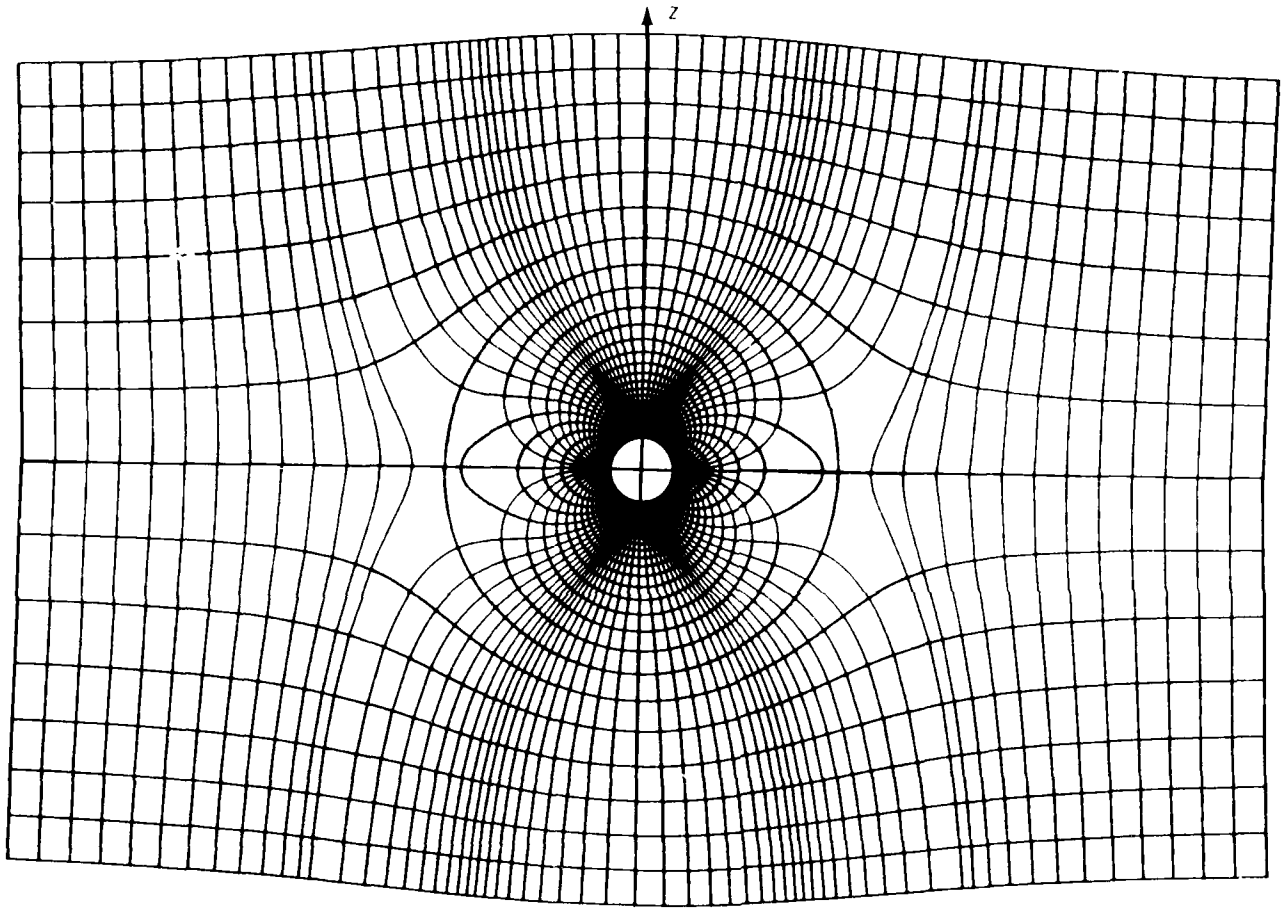

Figure 2. ζ_1 and ζ_2 contours for $k^{1/3} = 6\ R_e$. The earth is indicated by the circular area in the middle of the figure. The z-axis is aligned with the geomagnetic dipole axis in this example.

been chosen here is $6R_e$. The particular numerical algorithm employed in solving for the positive roots of P(r) was the Newton-Raphson method. In addition, the following constraints have been adhered to in selecting the ζ_1 and ζ_2 contour values for this mesh.

a) Cells on the surface of the earth at a colatitude of 15° have dimension ~ 100 km × 100 km.

b) The dimensions of successive cell boundaries along the z-axis moving away from the earth increase by 15% until a dimension equal to R_e is reached whereupon the rate of increase is reduced to zero.

c) In the upper hemisphere, the dimensions of successive cell boundaries along the surface of the earth are increased by 15% moving both clockwise and counter-clockwise from a colatitude of 15°. Boundaries in the lower hemisphere are obtained by reflection in the x-y plane.

d) The dimensions of successive cell boundaries along the y-axis to the right of the circular boundary increase by 15% until a dimension equal to R_e is attained whereupon the rate of increased is decreased to zero.

These constraints have been imposed in an attempt to realistically meet the requirements of an MHD code designed to simulate the behavior of a [illegible] magnetospheric plasma. Such a code should be capable of fine resolution in the vicinity of the auroral oval and at the same time be able to resolve the gross features of magnetospheric current systems. The [illegible] of the rate of increase of successive cell boundaries is [illegible] by the need to minimize the total number of cells in the mesh (which [illegible] the amount of computer storage required by the code) while

11	2	$-Z_2^2$	0	-3	$-2(Z_1^2-Z_2^2)$	0	0	$-(Z_1+Z_2)$	0	1
	2	$2-Z_2^2$	$2-Z_2^2$	$-1-Z_2^2$	$-1-2Z_1^2+Z_2^2$	$-1-2Z_1^2+Z_2^2$	$-1-2Z_1^2+Z_2^2$	$-1-3Z_2^2$	$-1-3Z_1^2$	$-3Z_1^2$
	2	$4-Z_2^2$	$6-2Z_2^2$	$5-3Z_2^2$	$4-2Z_1^2-2Z_2^2$	$3-4Z_1^2-Z_2^2$	$2-6Z_1^2$	$1-9Z_1^2$	$\underline{-12Z_1^2}$	
	2	$6-Z_2^2$	$12-3Z_2^2$	$17-6Z_2^2$	$21-2Z_1^2-8Z_2^2$	$24-6Z_1^2-9Z_2^2$	$26-12Z_1^2-9Z_2^2$	$\underline{27-21Z_1^2-9Z_2^2}$		
	2	$8-Z_2^2$	$20-4Z_2^2$	$37-10Z_2^2$	$58-2Z_1^2-18Z_2^2$	$82-8Z_1^2-27Z_2^2$	$\underline{108-20Z_1^2-36Z_2^2}$			
	2	$10-Z_2^2$	$30-5Z_2^2$	$67-15Z_2^2$	$125-2Z_1^2-33Z_2^2$	$\underline{207-10Z_1^2-60Z_2^2}$				
	2	$12-Z_2^2$	$42-6Z_2^2$	$109-21Z_2^2$	$\underline{234-2Z_1^2-54Z_2^2}$					
	2	$14-Z_2^2$	$56-7Z_2^2$	$\underline{165-28Z_2^2}$						
	2	$16-Z_2^2$	$\underline{72-8Z_2^2}$							
	2	$\underline{18-Z_2^2}$								
	2									

Figure A-2. Horner's Method applied to the polynomial $\tilde{\tilde{P}}(R)$

1	1	0	$-(Z_1^2+Z_2^2)$	0	0	$-2(Z_1^2-Z_2^2)$	[illegible]	0	$-Z_2^2$	2
	1	1	$-(Z_1^2+Z_2^2)+1$	$-(Z_1^2+Z_2^2)+1$	$-(Z_1^2+Z_2^2)+1$	$-3Z_1^2+Z_2^2+1$	$-3Z_1^2+Z_2^2-2$	$-3Z_1^2+Z_2^2-2$	$-3Z_1^2-2$	$-3Z_1^2$
	1	2	$-(Z_1^2+Z_2^2)+3$	$-2(Z_1^2+Z_2^2)+4$	$-3(Z_1^2+Z_2^2)+5$	$-6Z_1^2-2Z_2^2+6$	$-9Z_1^2-Z_2^2+4$	$-12Z_1^2+2$	$-15Z_1^2$	
	1	3	$-(Z_1^2+Z_2^2)+6$	$-3(Z_1^2+Z_2^2)+10$	$-6(Z_1^2+Z_2^2)+15$	$-12Z_1^2-8Z_2^2+21$	$-21Z_1^2-9Z_2^2+25$	$-33Z_1^2-9Z_2^2+2$		
	1	4	$-(Z_1^2+Z_2^2)+10$	$-4(Z_1^2+Z_2^2)+20$	$-10(Z_1^2+Z_2^2)+35$	$-22Z_1^2-18Z_2^2+56$	$-43Z_1^2-27Z_2^2+81$			
	1	5	$-(Z_1^2+Z_2^2)+15$	$-5(Z_1^2+Z_2^2)+35$	$-15(Z_1^2+Z_2^2)+70$	$-37Z_1^2-33Z_2^2+126$				
	1	6	$-(Z_1^2+Z_2^2)+21$	$-6(Z_1^2+Z_2^2)+56$	$-21(Z_1^2+Z_2^2)+126$					
	1	7	$-(Z_1^2+Z_2^2)+28$	$-7(Z_1^2+Z_2^2)+84$						
	1	8	$-(Z_1^2+Z_2^2)+36$							
	1	9								
	1									

Figure A-1. Horner's Method applied to the polynomial $\tilde{P}(R)$.

The first substitution transforms the equation $\tilde{P}(R)=0$ into the equation $\tilde{\tilde{P}}(R')=0$ with

$$\tilde{\tilde{P}}(R') = 2R'^9 - Z_2^2R'^8 - 3R'^6 - 2(Z_1^2-Z_2^2)R'^5 - (Z_1^2+Z_2^2)R'^2 + 1 \ . \quad \text{(A-7)}$$

As before, implementing the next two substitutions means rewriting $\tilde{\tilde{P}}(R')$ as a polynomial in $R''' = R'-1$:

$$\tilde{\tilde{P}}(R') = \sum_{n=0}^{9} h_n(Z_1, Z_2)\ (R'-1)^n \ . \quad \text{(A-8)}$$

This polynomial may also be shown (see below), to possess exactly one variation of sign for all Z_1 and Z_2, $Z_1 \neq 0$. Again by Descartes' Rule of Signs, this means that $\tilde{\tilde{P}}(R')$ has one and only one root greater than unity for each Z_1 and Z_2, $Z_1 \neq 0$. This in turn implies that $\tilde{P}(R)$ has one and only one positive root less than unity. Hence, $P(r)$ has one and only one root less than $k^{1/3}$ for each Z_1 and Z_2, $Z_1 \neq 0$. Since $r=k^{1/3}$ is not a root of $P(r)$ for $\xi_1 \neq 0$, the assertion that $P(r)$ has only two positive roots - one less than and the other greater than $k^{1/3}$ - will have been demonstrated once it has been shown that the coefficients $\{a_n\}$ and $\{h_n\}$, for $0 \leq n \leq 9$, possess one and only one variation of sign for arbitrary Z_1 and Z_2, $Z_1 \neq 0$.

One way to establish this property of the coefficients a_n, h_n is to calculate explicitly these quantities using Horner's Method. Figures A-1 and A-2 show the results of applying this algorithm to the polynomials $\tilde{P}(R)$ and $\tilde{\tilde{P}}(R)$ respectively. The required coefficients, listed in Table 1 for convenience, are given by the underlined terms in these Figures. Consider first the a_n's. a_9 and a_8 are positive while a_1 and a_0

of the initial substitutions in this sequence. One particularly advantageous choice is that set of substitutions which results in a translation of R by unity. This set of substitutions is given by

$$R = \frac{1}{R'} + 1 \tag{A-4a}$$

$$R' = 1/R'' \tag{A-4b}$$

which leads to

$$R = R'' + 1 \ . \tag{A-4c}$$

This choice is intuitively appealing because R=1 corresponds to $r=k^{1/3}$, the radial value for which the character of the ξ-coordinate system changes from being dipolar to being cylindrical. More importantly, the polynomial $\tilde{P}(R)$ rewritten as a polynomial in $R''=R-1$,

$$\tilde{P}(R) = \sum_{n=0}^{9} a_n(Z_1, Z_2)\ (R-1)^n \ , \tag{A-5}$$

may be shown to possess exactly one variation of sign for all Z_1 and Z_2, $Z_1 \neq 0$ (see below). By Descartes' Rule of Signs, this means that $\tilde{P}(R)$, has one and only one root R_0 which satisfies $(R_0-1)>0$, i.e., P(r) has one and only one root <u>greater</u> than $k^{1/3}$. To find the number of positive roots of P(r) <u>less</u> than $k^{1/3}$, consider the substitutions

$$R = \frac{1}{R'} \tag{A-6a}$$

$$R' = \frac{1}{R''} + 1 \tag{A-6b}$$

$$R'' = \frac{1}{R''} \tag{A-6c}$$

is a real polynomial with the first negative coefficient preceded by k coefficients which are positive or zero, and if G denotes the greatest of the absolute values of the negative coefficients, then each positive root is less than $1 + (\frac{G}{a_0})^{1/k}$.

The mathematical armada assembled above may now be brought to bear upon the problem of analyzing the positive roots of P(r). It is convenient to first scale P(r) by k^3.

$$\tilde{P}(R) \equiv \frac{P(r)}{k^3}$$

$$= R^9 - (Z_1^2+Z_2^2)R^7 - 2(Z_1^2-Z_2^2)R^4 - 3R^3 - Z_2^2R+2 \qquad \text{(A-2)}$$

with

$$R \equiv \frac{r}{k^{1/3}} \quad , \qquad \text{(A-3a)}$$

$$Z_1 \equiv \frac{\xi_1}{k^{1/3}} \quad , \qquad \text{(A-3b)}$$

and

$$Z_2 \equiv \frac{\xi_2}{k^{1/3}} \quad . \qquad \text{(A-3c)}$$

Clearly R_0 is a root of $\tilde{P}(R)$ if and only if $r_0 \equiv k^{1/3} R_0$ is a root of P(r). Hence, the objective of this Appendix can be accomplished by studying the positive roots of $\tilde{P}(R)$. As suggested above, one way to proceed in this study is to apply a sequence of the substitutions prescribed by Vincent's Theorem to $\tilde{P}(R)$ until one arrives upon a polynomial with no more than one variation of sign. The amount of labor required to pursue this approach can be minimized by a judicious (or perhaps fortuitous!) choice

The binominal theorem implies that this polynominal can be written as a polynomial of degree n in (x-c):

$$f(x) = A_n (x-c)^n + A_{n-1} (x-c)^{n-1} + \ldots + A_0 .$$

Horner's Method is an algorithm for calculating the coefficients A_i. It works as follows:

> First calculate A_0. Do this by using synthetic division to divide (x-c) into f(x). The result will be a polynomial, $f_1(x)$, of degree n-1 in x and a remainder which must be A_0. Now divide $f_1(x)$ by (x-c) again using synthetic division. The result is a polynomial, $f_2(x)$, of degree n-2 in x and a remainder which must be A_1. This sequence is repeated for a total of n times. The final iteration produces the obvious result $A_n=a_n$. In practice, it is convenient to arrange the various polynomial coefficients occurring within this procedure in a superdiagonal array.The ith row of this array consists of the coefficients of $f_i(x)$ arranged from left to right in decreasing rank order with the last term being the coefficient A_i. An example of such an array is shown in Figure A-1.

The final result from the theory of equations which will be required in this Appendix is a theorem which bounds the positive roots of a real polynomial.

<u>Result 4</u>:

If

$$f(x) = a_n x^n + a_{n-1} x^{n-1} \ldots + a_0 = 0 , \qquad a_n > 0 ,$$

m is counted as m roots. Two consecutive terms of a real polynomial are said to present a variation of sign if their coefficients have unlike signs.

As an example, the polynomial Equation (A-1a) has two variations of sign if $\xi_1^2 \geq \xi_2^2$ and four variations of sign if $\xi_1^2 < \xi_2^2$. In the first case, Descartes' rule allows zero, two, or four positive roots. Clearly Descartes' Rule by itself will precisely determine the number of positive roots of a real polynomial only if the polynomial has no more than one variation of sign. The following result is therefore a very useful adjunct to Descartes' Rule.

Result 2: (Vincent's Theorem)

If an equation without multiple roots is transformed successively by the substitutions

$$x = a+1/y \ , \ y = b+1/z \ , \ z = c+1/t \ \ldots$$

where a, b, c, ... are arbitrary positive integers, the transformed equation, after a sufficiently large number of such transformations, possesses either no variations of sign or just one.

Descartes' Rule of Signs and Vincent's Theorem form the basis of a universally applicable method of isolating the positive roots of a real polynomial. In using this method it is helpful to have an algebraic algorithm for efficiently performing the transformations required by Vincents' Theorem. One such algorithm is known as Horner's Method.

Result 3: (Horner's Method)

Suppose

$$f(x) = a_n x^n + a_{n-1} x^{n-1} \ldots + a_0 \ .$$

PREVIOUS PAGE IS BLANK

APPENDIX

In this Appendix, it will be shown that the polynomial P(r) given by

$$P(r) = r^9 - (\xi_1^2+\xi_2^2)r^7 - 2k(\xi_1^2-\xi_2^2)r^4 - 3k^2r^3 - k^2\xi_2^2 r + 2k^3 \quad \text{(A-1a)}$$

has precisely two positive roots if $\xi_1 \neq 0$. One of these roots lies in the interval $(0, k^{1/3})$ and the other in the interval $(k^{1/3} + \sqrt{M})$ where

$$M = \max\left[(\xi_1^2+\xi_2^2)\ ,\ 2(\xi_1^2-\xi_2^2)\ ,\ 3k^{2/3}\right] .$$

As an immediate corollary of this result, it will also be shown that the polynomial

$$Q(r) = r^3 - \xi_2^2\, r + 2k \quad \text{(A-1b)}$$

has precisely two positive roots for $\xi_2^2 > 3k^{2/3}$. One of these is always less than $k^{1/3}$ and the other always greater than $k^{1/3}$. The demonstration depends crucially upon several results from the theory of equations which are stated below without proof. Proofs of these results may be found in references 10 and 11.

<u>Result 1</u>: "Descartes' Rule of Signs"

The number of positive real roots of a polynomial with real coefficients is either equal to the number of its variations of sign or is less than that number by a positive even integer. A root of multiplicity

REFERENCES

1. Hoerlin, H., "United States High-Altitude Test Experiences," LA-6405, Los Alamos Scientific Laboratory, October 1976.

2. Potemra, T. A., T. Iijima, and N. A. Saflekos, "Large-Scale Characteristics of Birkeland Currents," in Dynamics of the Magnetosphere, eds. S. I. Akasofu, pp. 165-199, D. Reidel, Hingham, Mass, 1979.

3. Keskinen, M. J., P. K. Chaturvedi, and S. L. Ossakow, "Parametric Excitation and Suppression of Convective Plasma Instabilities in the High Latitude F-Region Ionosphere," NRL Memorandum Report 5133, Naval Research Laboratory, July 14, 1983.

4. Rino, C. L., E. J. Fremouw, R. C. Livingston, M. D. Cousins, and B. C. Fair, "WIDEBAND Satellite Observations," DNA 4399F, SRI Project 3793, SRI International, June 1977.

5. Fremouw, E. J., "HILAT - A Prelaunch Overview," DNA TR81-276, Physical Dynamics Incorporated, Bellevue, Washington, 13 June 1983.

6. Fremouw, E. J., P. L. Leadabrand, R. C. Livingston, M. D. Cousins, C. L. Rino, B. C. Fair, and R. A. Long, "Early Results from the DNA WIDEBAND Satellite Experiment -- Complex Signal Scintillation," Radio Science 13, No. 1, pp 167-187, Jan-Feb 1978.

7. White, W. W., "Late-Time Plume Dynamics," presented 14 July 1981 at the Defense Nuclear Agency High Altitude Phenomenology Review Meeting. Also see, White, W. W., "A Brief Review of HANE Phenomenology" in Proceedings of the DNA HILAT/High Altitude Review Meeting, October 1983.

8. See Appendix B of Stagat, R. W., D. S. Sappenfield, and J. P. Incerti, "The SCENARIO Code: Modifications in Version II and the Striation Convection Theory," AFWL-TR-80-124, GBC 3-2-MRC-057, Mission Research Corporation, April 1983.

9. Morse, Philip M. and Herman Feshbach, Methods of Theoretical Physics, p 14, McGraw-Hill Book Co., New York, New York, 1953.

10. Uspensky, J. V., Theory of Equations, McGraw-Hill Book Co., New York, 1948.

11. Dickson, Leonard Eugene, First Course in Theory of Equations, John Wiley & Sons, Inc., New York, 1922.

in this scheme is generated using the ζ-coordinate system and therefore possesses the advantages and disadvantages described in the preceding paragraph, i.e., it is well tailored to the elongated geometry of the magnetosphere and allows simple solar wind boundary conditions, but it also requires the existence of a spherical interface which would probably require special treatment within an MHD simulation code.

accomodates both the dipolarity of the near earth magnetic field and the elongated structure of the magnetosphere at large distances. An example of this rejoining is shown in Figure 3c. This particular mesh may be completed in three dimensions, under the previously stated constraints regarding the azimuthal dimensions of cells, by setting the angular separation between successive azimuthal planes of the inner and outer meshes to 0.06 and 0.07 radians, respectively. Notice that the use of an azimuthal axis aligned along the earth-sun line allows the outer mesh to be much shorter in the sunward direction, than in the anti-sunward direction corresponding to the fact that the magnetospheric bow shock region is compressed toward the earth while the magnetotail is distended away from the earth. Also, the use of such an axis permits a simple specification of solar wind boundary conditions. An apparent disadvantage of the use of this type of hybrid mesh, for purposes of constructing an MHD simulation code, is the presence of a spherical surface (at $r = k^{1/3}$) upon which the boundaries of adjacent cells are not aligned. This surface would probably require special treatment within such a code if spurious numerical effects are to be avoided.

There are other ways to construct "hybrid" meshes using the ζ-coordinate system which should be mentioned briefly here for completeness. For example, instead of using the z' axis shown in Figure 3b as the azimuthal axis of the exterior mesh, one might use the z-axis of the ζ-coordinate system itself, now aligned along the magnetospheric axis of elongation. This choice would concentrate resolution in the equatorial regions of the mesh at the expense of resolution in the polar regions so that it does not seem to be as desirable an alternative as that pictured in Figure 3 for the high latitude problem of concern here. Another option is to generate the interior mesh of Figure 3 using a <u>spherical</u> coordinate system. The benefits of dipolarity are thereby relinquished in favor of the simplicity of a spherical geometry near the earth. The exterior mesh

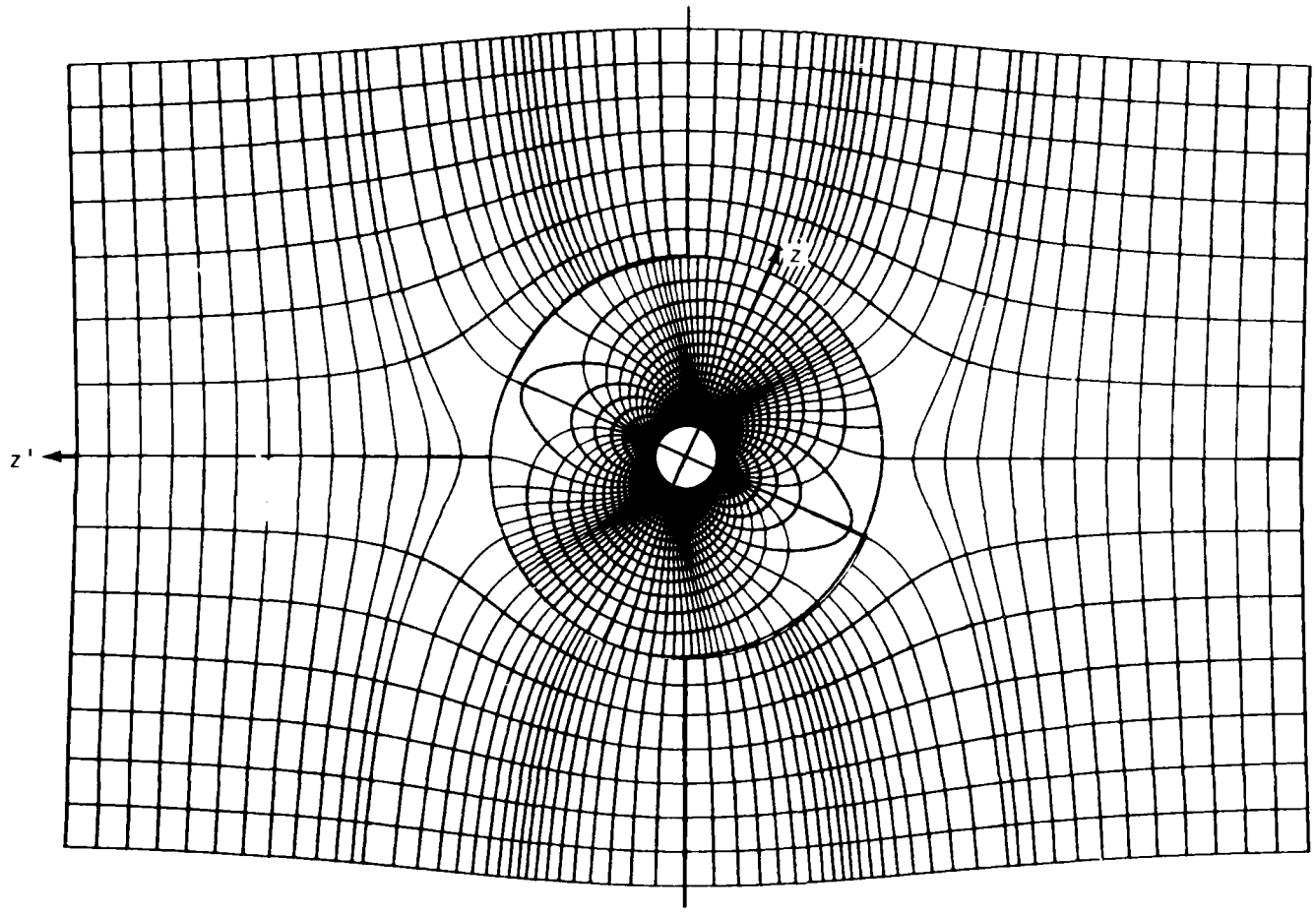

Figure 3c. An example of how Figures 3a and 3b might be rejoined to generate a complete mesh. The spherical nature of the interface at $r=k^{1/3}$ allows the z and z' axes to be oriented arbitrarily with respect to one another.

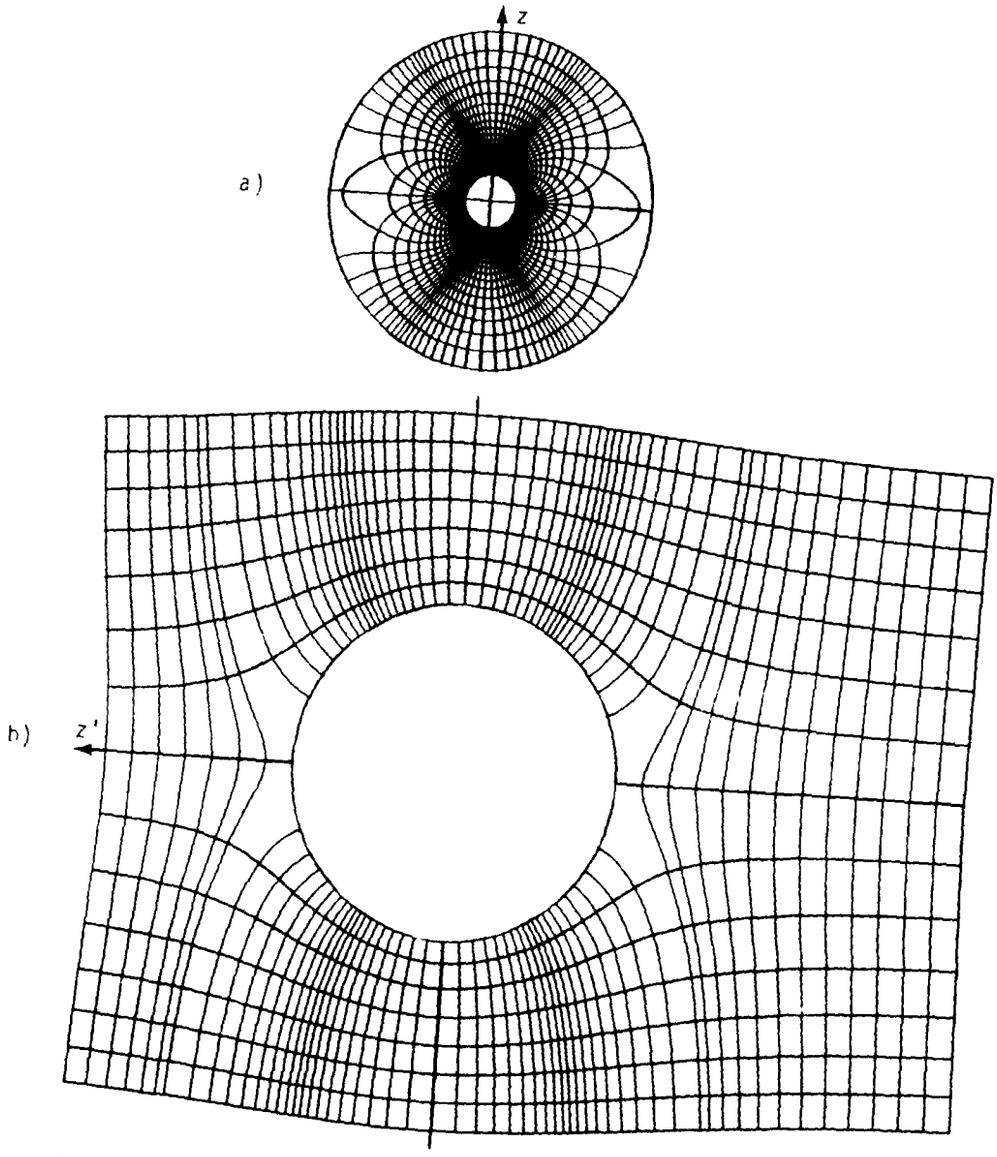

Figure 3. An illustration of the use of two azimuthal axes in generating a mesh based upon the ζ-coordinate system.

3a. The portion of the mesh of Figure 2 which lies within the circle of radius $k^{1/3}$. The z-axis is chosen to be along the geomagnetic dipole axis.

3b. The portion of the mesh of Figure 2 which lies outside the circle of radius $k^{1/3}$. The azimuthal axis z' defined in the text would be taken as the axis of elongation of the magnetosphere.

maintaining acceptable bounds upon numerical error arising from off-center differencing. To complete the mesh in three dimensions, the contours of of Figure 2 must be rotated azimuthally. In order for the azimuthal dimensions of cells at the periphery of the mesh to be limited to $\sim R_e$ and to maintain 100 km resolution in the vicinity of the auroral oval, the angle between successive azimuthal planes in the full three dimensional mesh should be taken equal to ~ 0.05 radian.

The three dimensional mesh described above fails to make optimal use of the cylindrical character of the ζ-coordinate system at large distances because the z-axis of this mesh is aligned with the geomagnetic dipole axis rather than with the earth-sun line. This problem may be alleviated by using the ζ-coordinate system to generate a mesh with two <u>different</u> azimuthal axes. One way to do this is illustrated in Figure 3. In Figure 3a, the dipolar part of the mesh of Figure 2, i.e., that part which lies within the sphere of radius $k^{1/3}$, has been isolated and is shown with its azimuthal axis directed along the geomagnetic dipole axis, just as it is in Figure 2. In Figure 3b, on the other hand, the remainder of the mesh exterior to the sphere of radius $k^{1/3}$, is pictured with another axis, called z', being used to define the azimuth. z' is the azimuthal axis of a coordinate system $\{\zeta_i'\}$ which is related to the ζ-coordinate system by a simple colatitudinal translation:

$$\zeta_1' = (r - k/r^2) \sin \theta \ , \tag{4-13}$$

$$\zeta_2' = (r^2 + 2k/r) \cos \theta \ , \tag{4-14}$$

and

$$\zeta_3' = \phi \ . \tag{4-15}$$

Since the meshes of Figures 3a and 3b both possess a spherical boundary at $r = k^{1/3}$, they may be easily rejoined to create a "hybrid" mesh which

Table 1. The coefficients $\{a_n\}, \{b_n\}$ calculated by Horner's Method.

$a_0 = -3Z_1^2$	$b_0 = -3Z_1^2$
$a_1 = -15Z_1^2$	$b_1 = -12Z_1^2$
$a_2 = -9(Z_1^2+Z_2^2) - 24Z_1^2 + 27$	$b_2 = 27-21Z_1^2 - 9Z_2^2$
$a_3 = -27(Z_1^2+Z_2^2) - 16Z_1^2 + 81$	$b_3 = 108 - 20Z_1^2 - 36Z_2^2$
$a_4 = -33(Z_1^2+Z_2^2) - 4Z_1^2 + 126$	$b_4 = 207 - 10Z_1^2 - 60Z_2^2$
$a_5 = -21(Z_1^2+Z_2^2) + 126$	$b_5 = 234 - 2Z_1^2 - 54Z_2^2$
$a_6 = -7(Z_1^2+Z_2^2) + 84$	$b_6 = 165 - 28Z_2^2$
$a_7 = -(Z_1^2+Z_2^2) + 36$	$b_7 = 72 - 8Z_2^2$
$a_8 = 9$	$b_8 = 18 - Z_2^2$
$a_9 = 1$	$b_9 = 2$

are negative for $Z_1 \neq 0$. Thus, there is always at least one variation of sign presented by these coefficients. It is easy to see that there are no more variations of sign for arbitrary Z_1 and Z_2 with $Z_1 \neq 0$ by considering possibilities (a)-(f), below, regarding the magnitude of the quantity $Z_1^2+Z_2^2$.

(a) $Z_1^2+Z_2^2 > 36$

In this case a_7 is obviously negative. In addition, each of the terms a_n, $n<7$, are also negative so that there is only one variation of sign presented by the coefficients $\{a_n\}$ for this case.

(b) $12 < Z_1^2+Z_2^2 \leq 36$

Now a_7 is non-negative, but a_n for $n \leq 6$ is negative definite. Again there is only one variation of sign.

(c) $6 < Z_1^2+Z_2^2 \leq 12$

a_7 and a_6 are both non-negative while a_n for $n \leq 5$ is negative definite. There is only one variation of sign.

(d) $\frac{126}{33} < Z_1^2+Z_2^2 \leq 6$

a_7, a_6, and a_5 are all non-negative while a_n for $n \leq 4$ is negative definite. There is only one variation of sign.

(e) $3 < Z_1^2+Z_2^2 < \frac{126}{33}$

a_7, a_6, a_5, are non-negative while a_3 and a_2 are negative definite. Hence, regardless of the sign of a_4, there is only one variation of sign presented by the sequence of coefficients $\{a_n\}$.

(f) $0 < Z_1^2+Z_2^2 \leq 3$

In this case, a_n for $n \geq 4$ is positive. Also

$a_3-a_2 = -18(Z_1^2+Z_2^2) + 8Z_1^2 + 54 > 0$,

so again there can only be one variation of sign.

For arbitrary Z_1 and Z_2 with $Z_1 \neq 0$ the quantity $(Z_1^2+Z_2^2)$ must fall within one of the intervals (a) - (f). Hence it has been shown that the sequence of coefficients $\{a_n\}$ presents only one variation of sign for all Z_1, Z_2, $Z_1 \neq 0$. Now consider the coefficients $\{b_n\}$. b_0 and b_1 are negative while b_9 is positive, so that there is at least one variation of sign presented by the coefficients of $\tilde{P}$. To see that there is in fact <u>only</u> one variation of sign presented by these coefficients, proceed as above to consider several possibilities regarding the value of Z_2^2, with Z_1^2 arbitrary but non-vanishing.

(a) $Z_2^2 > 18$

In this case, b_n for $n \leq 8$ is negative so that there is clearly only one variation of sign.

(b) $9 \leq Z_2^2 \leq 18$

Now b_9 and b_8 are non-negative while b_n for $n \leq 7$ is negative definite. Again there is only one variation of sign.

(c) $\frac{165}{28} < Z_2^2 \leq 9$

b_9, b_8 and b_7 are non-negative and b_n, for $n \leq 6$ is negative; there is only one variation of sign.

(d) $3 < Z_2^2 \leq \frac{165}{28}$

b_9, b_8, b_7, and b_6 are non-negative while b_n for $n \leq 3$ is negative definite. Also

$$b_5 - b_4 = 27 + 8Z_1^2 + 6Z_2^2 > 0 \ ,$$

so that $b_5 > b_4$ for all Z_1, Z_2. Hence, there can be only one variation of sign for this case also.

(e) $Z_2^2 \leq 3$

For this case, the b_n's satisfy the inequality

$$b_5 > b_4 > b_3 > b_2 .$$

The first part of this chain has already been established above. To demonstrate the remaining parts, compute the differences

$$b_4 - b_3 = 99 + 10Z_1^2 - 24Z_2^2$$

and

$$b_3 - b_2 = 81 + Z_1^2 - 27Z_2^2 ,$$

which are both positive definite for $Z_2^2 \leq 3$ and $Z_1 \neq 0$. With this inequality and the observation that b_9, b_8, b_7, and b_6 are positive for $Z_2^2 \leq 3$, it is evident that there is only one variation in sign in the coefficients $\{b_n\}$ for this case also.

It has now been shown that $P(r)$ has precisely two positive roots for $Z_1 \neq 0$. One of these roots lies within the interval $(0, k^{1/3})$, and the other lies outside of this interval. An upper bound for the larger root can be obtained by using Result 4 above. It immediately follows by inspection of $\tilde{P}(R)$ that the larger root must lie in the interval $(k^{1/3}, k^{1/3} + \sqrt{M})$ with

$$M \equiv \max(\xi_1^2 + \xi_2^2,\ 2(\xi_1^2 - \xi_2^2),\ 3k^{2/3}) .$$

This is one of the results which was to be demonstrated in this Appendix.

To derive the other result, namely that the polynomial $Q(r)$ (Equation A-1b) has precisely two postive roots - one less than and the other greater than $k^{1/3}$, if $|\xi_2| > \sqrt{3}\, k^{1/3}$, note first that

$$P(r)\Big|_{\xi_1=0} = (r^3 - k)^2\, Q(r) \qquad \text{(A-9)}$$

This follows by direct multiplication or by inspection of Equation (4-10) in the text. Equation (A-9) can be rewritten

$$P(r)\Big|_{\xi_1=0} = (r-k^{1/3})^2\,(r^2+rk^{1/3}+k^{2/3})^2\,Q(r) \qquad \text{(A-10)}$$

Since the polynomial comprising the middle factor of the right hand side of Equation (A-10) has no variation of sign, it can have no positive roots. Therefore, the positive roots of $Q(r)$ are the same as the positive roots of $P(r)\big|_{\xi_1=0}$ with the factor $(r-k^{1/3})^2$ removed. Thus, the above assertion regarding $Q(r)$ can be demonstrated by showing that the coefficients $\{a_n\}_{n=2,9}$ and $\{b_n\}_{n=2,9}$ above present one and only one variation of sign for $\xi_1=0$, $|\xi_2|>\sqrt{3}\,k^{1/3}$. That this is so can be seen immediately from the above discussion regarding these coefficients.

DISTRIBUTION LIST

DEPARTMENT OF DEFENSE

Asst to the Secy of Defense
Atomic Energy
ATTN: Executive Assistant

Defense Advanced Rsch Proj Agency
ATTN: GSD, R. Alewene
ATTN: STO, W. Kurowski

Defense Nuclear Agency
ATTN: RAAE, P. Lunn
ATTN: RAAE, K. Schwartz
ATTN: RAEE
3 cy ATTN: RAAE
4 cy ATTN: STTI-CA

Defense Technical Information Center
12 cy ATTN: DD

Deputy Under Secy of Defense
Comm, Cmd, Cont & Intell
ATTN: Dir of Intell Sys

Field Command, DNA, Det 1
Lawrence Livermore National Lab
ATTN: FC-1

Field Command, DNA
ATTN: FCPR
ATTN: FCTT, W. Summa
ATTN: FCTXE

Joint Chiefs of Staff
ATTN: C3S
ATTN: C3S Evaluation Office, HD00

DEPARTMENT OF THE ARMY

US Army Electronics R&D Command
ATTN: DELAS-EO, F. Niles

Harry Diamond Laboratories
ATTN: DELHD-NW-R, R. Williams
2 cy ATTN: DELHD-NW-P

US Army Nuclear & Chemical Agency
ATTN: Library

US Army Satellite Comm Agency
ATTN: Document Control

US Army Communications R&D Command
ATTN: DRDCO-COM-RY, W. Kesselman

DEPARTMENT OF THE NAVY

Naval Ocean Systems Center
ATTN: Code 532
ATTN: Code 5322, M. Paulson
ATTN: Code 5323, J. Ferguson

Naval Space Surveillance System
ATTN: J. Burton

Office of Naval Research
ATTN: Code 412, W. Condell

DEPARTMENT OF THE NAVY (Continued)

Naval Research Laboratory
ATTN: Code 4108, E. Szuszewicz
ATTN: Code 4187
ATTN: Code 4700
ATTN: Code 4700, S. Ossakow
ATTN: Code 4720, J. Davis
ATTN: Code 4780
ATTN: Code 6700
ATTN: Code 7500, B. Wald
ATTN: Code 7950, J. Goodman

DEPARTMENT OF THE AIR FORCE

Air Force Geophysics Laboratory
ATTN: CA, A. Stair
ATTN: LIS, J. Buchau
ATTN: LYD, K. Champion
ATTN: OPR, H. Gardiner
ATTN: OPR-1
ATTN: R. Babcock
ATTN: R. O'Neil

Air Froce Space Technology Ctr
ATTN: YH

Air Force Weapons Laboratory
ATTN: NTN
ATTN: SUL

Air University Library
ATTN: AUL-LSE

Asst Chief of Staff, Studies & Analysis
ATTN: AF/SASC, C. Rightmeyer

Ballistic Missile Office/DAA
ATTN: ENSN
ATTN: ENSN, W. Wilson
ATTN: SYC, D. Kwan

Deputy Chief of Staff, Rsch, Dev & Acq
ATTN: AF/RDQI

Electronic Systems Division/SC
ATTN: SCS-1E
ATTN: SCS-2, G. Vinkels

Rome Air Development Center
ATTN: EEP, J. Rasmussen
ATTN: EEPS, P. Kossey

Space Command
ATTN: DC, T. Long

OTHER GOVERNMENT AGENCIES

Department of Commerce
ATTN: Sec Ofc for R. Moore

Department of Commerce
ATTN: R. Grubb

Institute for Telecommunications Sciences
ATTN: A. Jean
ATTN: L. Berry
ATTN: W. Utlaut

PREVIOUS PAGE IS BLANK

NATO

NATO School, SHAPE
ATTN: US Documents Officer

DEPARTMENT OF ENERGY CONTRACTORS

University of California
Lawrence Livermore National Lab
ATTN: L-31, R. Hager
ATTN: Tech Info Dept Library

Los Alamos National Laboratory
ATTN: D. Sappenfield
ATTN: D. Simons
ATTN: G-6, E. Jones
ATTN: MS 670, J. Hopkins
ATTN: J. Wolcott
ATTN: MS 664, J. Zinn
ATTN: R. Jeffries
ATTN: T. Kunkle, ESS-5

Sandia National Laboratories
ATTN: D. Dahlgren
ATTN: D. Thornbrough
ATTN: Org 1231, R. Backstrom
ATTN: Org 1250, W. Brown
ATTN: Org 4231, T. Wright
ATTN: Space Project Div
ATTN: Tech Library 3141

DEPARTMENT OF DEFENSE CONTRACTORS

Berkeley Rsch Associates, Inc
ATTN: C. Prettie
ATTN: J. Workman
ATTN: S. Brecht

EOS Technologies, Inc
ATTN: B. Gabbard
ATTN: W. Lelevier

JAYCOR
ATTN: J. Sperling

Johns Hopkins University
ATTN: C. Meng
ATTN: J. Phillips
ATTN: J. Newland
ATTN: K. Potocki
ATTN: R. Stokes
ATTN: T. Evans

Kaman Tempo
ATTN: B. Gambill
ATTN: DASIAC
ATTN: W. McNamara

Kaman Tempo
ATTN: DASIAC

Lockheed Missiles & Space Co, Inc
ATTN: J. Kumer
ATTN: R. Sears

M I T Lincoln Lab
ATTN: D. Towle
ATTN: N. Doherty
ATTN: V. Vitto

R&D Associates
ATTN: B. Yoon

DEPARTMENT OF DEFENSE CONTRACTORS

Maxim Technologies, Inc
ATTN: E. Tsui
ATTN: J. Marshall
ATTN: R. Morgenstern

Mission Research Corp
ATTN: C. Lauer
ATTN: D. Knepp
ATTN: F. Fajen
ATTN: F. Guigliano
ATTN: G. McCartor
ATTN: R. Bigoni
ATTN: R. Bogusch
ATTN: R. Dana
ATTN: R. Hendrick
ATTN: R. Kilb
ATTN: S. Gutsche
ATTN: Tech Library
2 cy ATTN: D. Maloof
2 cy ATTN: W. White
5 cy ATTN: Document Control

Physical Dynamics, Inc
ATTN: E. Fremouw
ATTN: J. Secan

Physical Research, Inc
ATTN: K. Schueter
ATTN: R. Deliberis
ATTN: T. Stephens

Physical Research, Inc
ATTN: J. Devore
ATTN: J. Thompson

R&D Associates
ATTN: C. Greifinger
ATTN: F. Gilmore
ATTN: G. St Cyr
ATTN: H. Ory
ATTN: M. Gantsweg
ATTN: P. Haas
ATTN: R. Turco
ATTN: W. Karzas
ATTN: W. Wright

SRI International
ATTN: A. Burns
ATTN: C. Rino
ATTN: D. McDaniels
ATTN: D. Neilson
ATTN: G. Price
ATTN: G. Smith
ATTN: J. Petrickes
ATTN: J. Vickrey
ATTN: M. Baron
ATTN: R. Leadabrand
ATTN: R. Livingston
ATTN: R. Tsunoda
ATTN: V. Gonzales
ATTN: W. Chesnut
ATTN: W. Jaye

Visidyne, Inc
ATTN: C. Humphrey
ATTN: H. Smith
ATTN: J. Carpenter
ATTN: O. Shepard
ATTN: W. Reidy

END

DATE
FILMED

9-85